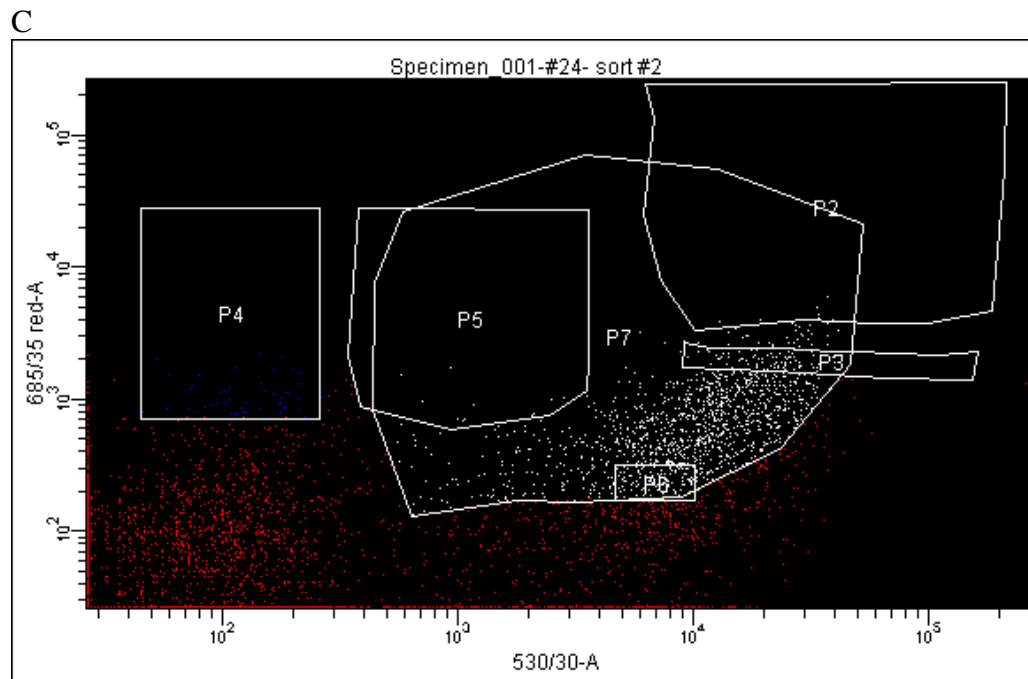
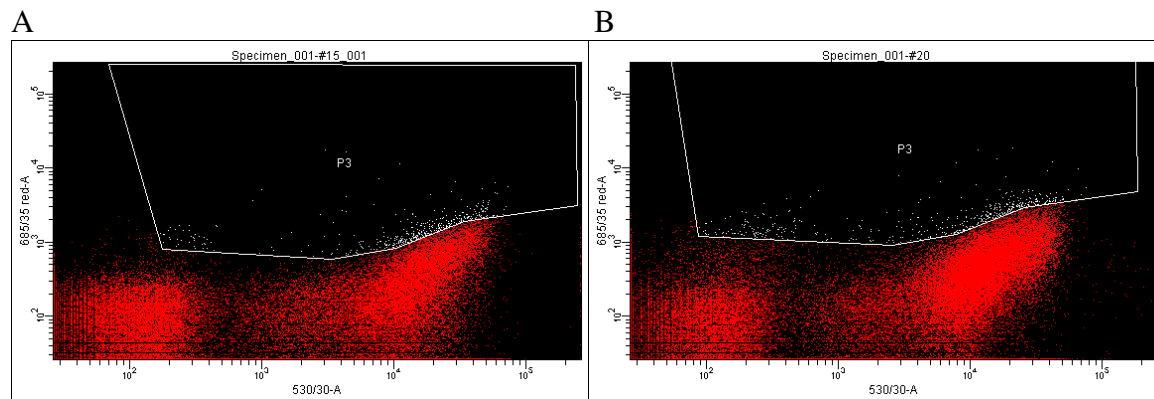


Supporting Information for “A Variable Light Domain Fluorogen Activating Protein Homodimerizes to Activate Dimethylindole Red”

Supporting Information Figure S1 Directed evolution FACS enrichment data of M8V_L and M8V_HV_L.

Directed evolution FACS enrichments of M8V_HV_L with DIR.(Panels A-C)

Panel A. First sort of a library of yeast cells expressing error prone PCR mutants of M8V_HV_L. The x-axis indicates the cell surface expression of the scFvs as determined by fluorescent c-myc epitope labeling with anti-cmyc antibody (Roche) and Alexa 488 (Invitrogen). The y-axis shows the increasing fluorescence signal of the yeast library interrogated with 0.5nM DIR. Gate P3 (white box and white cells) was drawn to isolate and expand 0.5% of the total library yeast library with the greatest DIR fluorescence.



Panel B. Second sort of a library of yeast cells expressing error prone PCR mutants of M8V_HV_L. The x-axis indicates the cell surface expression of the scFvs as determined by fluorescent c-myc

epitope labeling with anti-cmyc antibody (Roche) and Alexa 488 (Invitrogen). The y-axis shows the increasing fluorescence signal of the yeast library interrogated with 0.25nM DIR. Gate P3 (white) was drawn to isolate and expand 0.5% of the total library yeast library with the greatest DIR fluorescence.

Panel C. Third sort of a library of yeast cells expressing error prone PCR mutants of M8V_HV_L. The x-axis indicates the cell surface expression of the scFvs as determined by fluorescent c-myc epitope labeling with anti-cmyc antibody (Roche) and Alexa 488 (Invitrogen). The y-axis shows the increasing fluorescence signal of the yeast library interrogated with 0.25nM DIR. Different gates were drawn in order to isolate single yeast cell that represented distinct populations with different expression and fluorescence profiles. For example, gate P2 (top right hand corner) was drawn to isolate clones with the greatest DIR fluorescence and scFv expression. Another example is gate P7 that was drawn around clones with strong DIR fluorescence but less robust yeast surface expression as indicated by reduced fluorescence from the c-myc epitope labeling. Clones were isolated from each of the 7 gates and plated as single cells onto yeast induction media containing plates with agar and 10nM DIR for visual inspection.

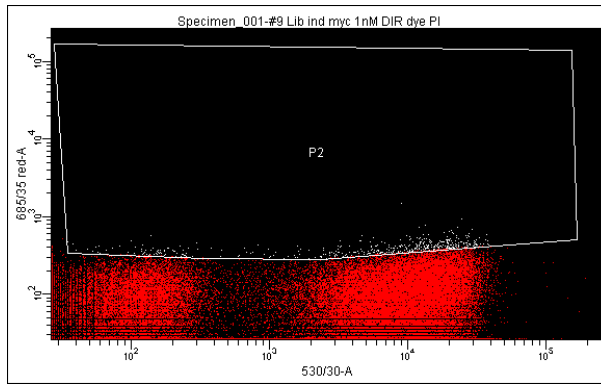
Directed Evolution FACS enrichments for M8V_L (Panels D-F)

Panel D. First sort of a library of yeast cells expressing error prone PCR mutants of M8V_L. The x-axis indicates the cell surface expression of the scFvs as determined by fluorescent c-myc epitope labeling with anti-cmyc antibody (Roche) and Alexa 488 (Invitrogen). The y-axis shows the increasing fluorescence signal of the yeast library interrogated with 1.0nM DIR. Gate P2 (white) was drawn to isolate and expand 0.5% of the total library yeast library with the greatest DIR fluorescence.

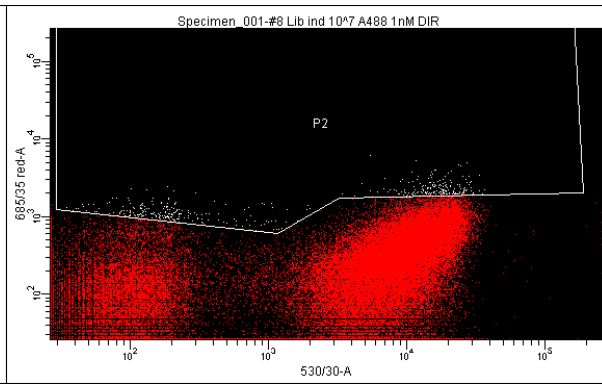
Panel E. Second sort of a library of yeast cells expressing error prone PCR mutants of M8V_L. The x-axis indicates the cell surface expression of the scFvs as determined by fluorescent c-myc epitope labeling with anti-cmyc antibody (Roche) and Alexa 488 (Invitrogen). The y-axis shows the increasing fluorescence signal of the yeast library interrogated with 1.0nM DIR. Gate P2 (white) was drawn to isolate and expand 0.5% of the total library yeast library with the greatest DIR fluorescence.

Panel F. Third sort of a library of yeast cells expressing error prone PCR mutants of M8V_L. The x-axis indicates the cell surface expression of the scFvs as determined by fluorescent c-myc epitope labeling with anti-cmyc antibody (Roche) and Alexa 488 (Invitrogen). The y-axis shows the increasing fluorescence signal of the yeast library interrogated with 1.0 nM DIR. Different gates were drawn in order to isolate single yeast cell that represented distinct populations with different expression and fluorescence profiles. For example, gate P3 was drawn to isolate clones with the greatest DIR fluorescence and scFv expression. Cells from each gate were plated as colonies containing single cells onto yeast induction media containing plates with agar and 10nM DIR for visual inspection.

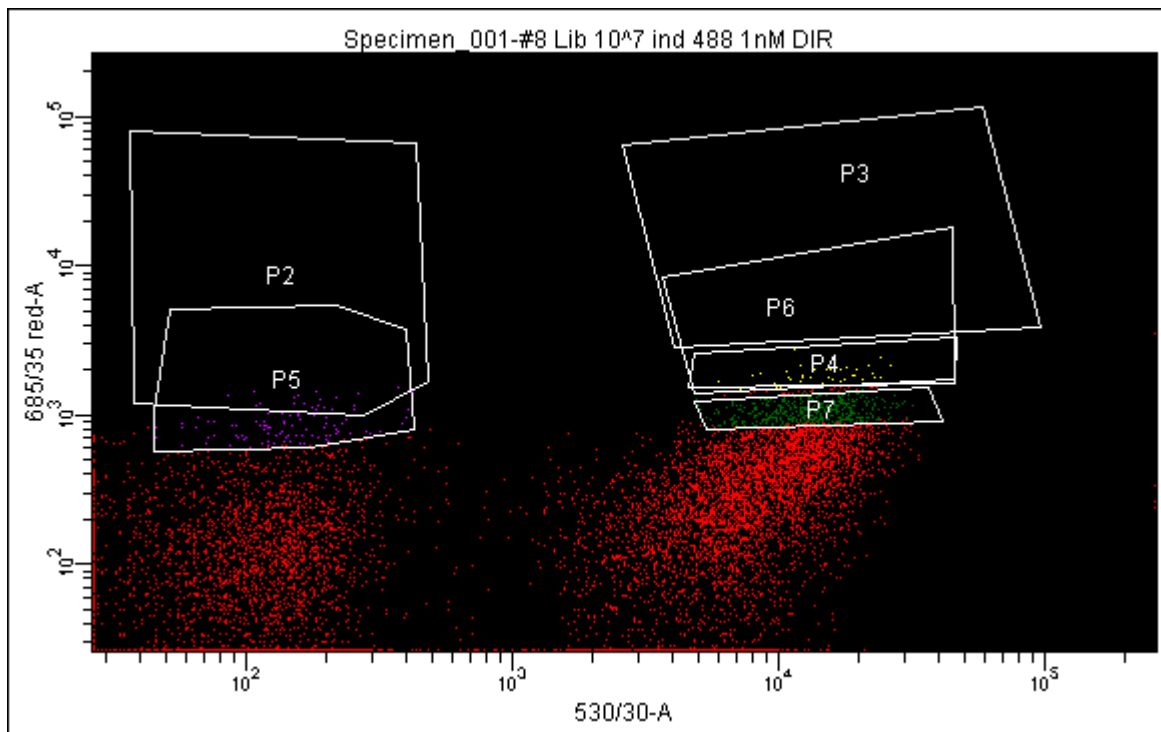
D



E



F

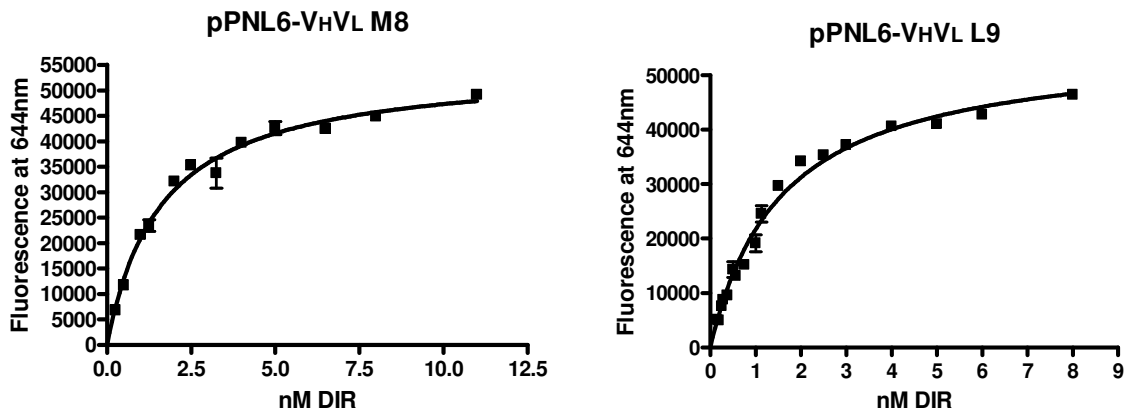


Supporting Information Figure S2. Characteristics of clones isolated from directed evolution of V_H-V_L M8 and M8V_L FAPs and fluorescence equilibrium affinity determinations on the yeast cell surface.

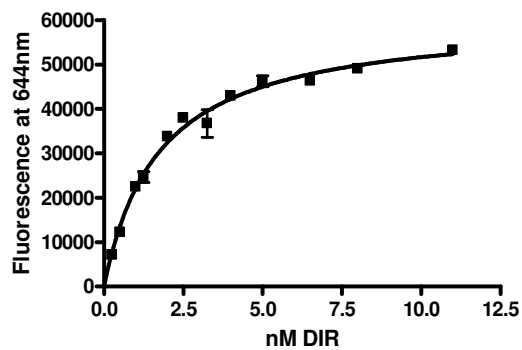
Table S2. Characteristics of FAPs before and after directed evolution.

Clone name	Format	surface K _D (nM)	Mutations in sequence different from wild type (V _H -V _L M8 or M8V _L)
M8	V _H -V _L	1.2 ± 0.2	
L9	V _H -V _L	1.6 ± 0.1	F ^{H29} S, W ^{H36} C, A ^{H93} V, I ^{H113i} T
Q9	V _L	1.9 ± 0.1	Q ^{L1} R, T ^{L14} I, D ^{L30} G, Q ^{L37} R, S ^{L55} P, F ^{L62} L, S ^{L80} P
J8	V _L -V _L	10.4 ± 1.4	VL#1: D ^{L83} N, K ^{L103} T, L ^{L107} S, I ^{L108i} T VL#2: S ^{L9} P, S ^{L32} P
M8V _L	V _L	1.8 ± 0.1	
A4	V _L	1.0 ± 0.2	S ^{L55} P

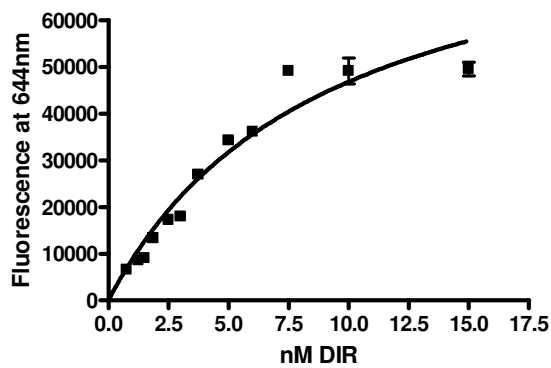
Affinity titrations represented in Table S2. Serial dilutions of DIR were added to 10⁶ yeast cells induced to display the protein of interest in buffer (PBS pH 7.4 with 2mM EDTA, 0.1% w/v Pluronic F-127). All pPNL6 titles on figures indicate yeast surface display clones with the clone name after the pPNL6. The yeast surface proteins (black squares) are shown. All measurements were performed in duplicate in 96 well black-bottom plates (Whatman) in Tecan Safire² fluorimeter and excited at 602nm. The fluorescence measurements of DIR titrations into 10⁶ uninduced yeast cells in buffer were subtracted from raw data prior to curve fitting. Fluorescence was recorded at 644nm and data analyzed using GraphPad fit to a one-site binding equation $y = F_{\max} * [X] / (K_d + [X])$, where [X] is the DIR concentration.



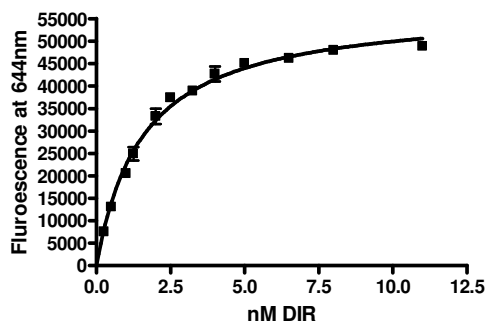
pPNL6-VL Q9



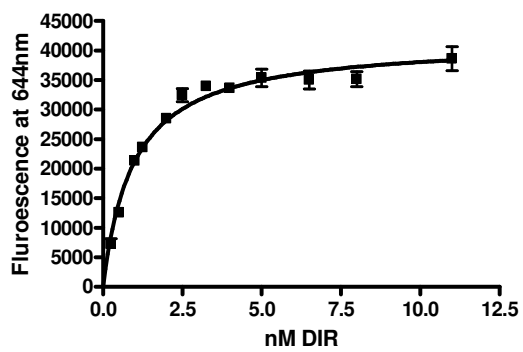
pPNL6-VLVL J8



pPNL6-M8VL



pPNL6-M8VL S^{L55P}



Supporting Information Figure S3. Amino acid sequence alignment of V_H-V_L M8 wild type (top) compared to clones isolated after directed evolution that contain both V_H and V_L domains. Clone names are listed on the left hand side with conserved residues shown as stars, conserved mutations listed by “:”, semi-conserved by “.”, and a blank space indicates no conserved match (ClustalW).

```

VHVL8      QVQLVESEGGVLVQPGGSLRLSCAASGFTFSSYWMSWVRQAPGKGLEGVATIKQDGSEKYY 60
L13       QVQLVESEGGVLVQPGGSLRLSCAASGFTFSSYWMSWVRQAPGKGLEGVATIKQDGSEKYY 60
L9        QVQLVESEGGVLVQPGGSLRLSCAASGFTFSSYWMSWVRQAPGKGLEGVATIKQDGSEKYY 60
O3        QVQLVESEGGVLVQPGGSLRLSCAASGFTFSSYWMSWVRQAPGKGLEGVATIKQDGSEKYY 60
P15      QVQLVESEGGVLVQPGGSLRLSCAASGFTFSSCWMSWVRQAPGKGLEGVATIKQDGSEKYY 60
O5       QVQLVESEGGVLVQPGGSLRLSCAASGFTFSSYWMSWVRQAPGKGLEGVATIKQDGSEKYY 60
K6       QVQLVESEGGVLVQPGGSLRLSCAASGFTFSSYWMSWVRQAPGKGLEGVATIKQDGSEKYY 60
R2       QVQLVESEGGVLVQPGGSLRLSCAASGFAFSSYWVSWVRQAPGKGLEGVATIKQDGSEKYY 60
          *****:****.*****: ** *: *****

VHVL8      VDSVKGRITISRDNAKNSLNRQINSLRAEDTAVYYCARDRLVRETGGDYRGLDLWGQGT 120
L13       VDSVKGRITISRDNAKNSLNRQINSLRAEDTAVYYCARDRLVRETGGDYRGLDLRGQGT 120
L9        VDSVKGRITISRDNAKNSLNRQINSLRAEDTAVYYCVRDLVRETGGDYRGLDLWGQGT 120
O3        VDSVKGRITISRDNAKNSLNRQINSLRAEDTAVYYCARDRLVRETGGDYRGLDLWGQGT 120
P15      VDSVKGRITISRDNAKNSLNRQINSLRAEDTAVYYCARDRLVRETGGDYRGLDLWGQGT 120
O5       VDSVKGRITISRDNAKNSLNRQINSLRAEDTAVYYCARDRLVRETGGDYRGLDLWGQGT 120
K6       VDSVKGRITISRDNAKNSLNRQINSLRAEDTAVYYCARDRLVRETGGDYRGLDLWGQGT 120
R2       VDSVKGRITISRDNAKNSLNRQINSLRAEDTAVYYCARDRPVRETGGDYRGLDLWGQGT 120
          *****.*** ***** ** *****

VHVL8      VTVSSASTKGPSGILGSGGGGSGGGGSGGGGSPVLTQSPSVSGTPGQKVTIFCSGSSSN 180
L13       VTVSSASTKGPSGILGSGGGGSGGGGSGGGGSPVLTQSPSVSGTPGQKVTIFCSGSSSN 180
L9        VTVSSASTKGPSGILGSGGGGSGGGGSGGGGSPVLTQSPSVSGTPGQKVTIFCSGSSSN 180
O3        VTVSSASTRGPSGILGSGGGGSGGGGSGGGGSPALTOQSPSVSGTPGQKVTIFCSGSSSN 180
P15      VTVSSASTRGPSGILGSGGGGSGGGGSGGGGSPALTOQSPSVSGTPGQKVTIFCSGSSSN 180
O5       VTVSSASTKGPSGILGSGGGGSGGGGSGGGGSPVLTQSPSVSGTPGQKVTIFCSGSSSN 180
K6       VTVSSASTKGPSGILGSGGGGSGGGGSGGGGSPVLTQSPSVSGTPGQKVTIFCSGSSSN 180
R2       VTVSSASTKGPSRILGSGGGGSGGGGSGGGGSPVLTQSPSVSGTPGQKVTIFCSGSSSN 180
          *****:*** *****.*****.***

VHVL8      VEDNSVYWYQQFPGTTPKVLIYNDDRSSGVPDRFSGSKSGTSASLAISGLRSEDEADYY 240
L13       VEDNSVYWYQQFPGTTPKVLIYNDDRSSGVPDRFSGSKSGTSASLAISGLRSEDEADYY 240
L9        VEDNSVYWYQQFPGTTPKVLIYNDDRSSGVPDRFSGSKSGTSASLAISGLRSEDEADYY 240
O3        VEDNSVYWYQQFPGTTPKVLIYNDDRSPGVPDRFSGSKSGTSASLAISGLRSEDEADYY 240
P15      VEDNSVYWYQQFPGTTPKVLIYNDDRSSGVPDRFSGSKSGTSASLAISGLRSEDEADYY 240
O5       VEDNSVYWYQQFPGTTPKVLIYNDDRSPGVPDRFSGSKSGTSASLAISGLRSEDEADYY 240
K6       VEDNSVYWYQQFPGTTPKVLIYNDDRSPGVPDRFSGSKSGTSASLAISGLRSEDEADYY 240
R2       VEDNSVYWYQQFPGATPKVLIYNDDRSPGVPDRFSGSKSGXSASLXISGLRSEDEADYY 240
          * *****:*****.***** ***** *****

VHVL8      CLSWDDSLNGWVFGGGTKVTVL 262
L13       CLSWDDSLNGWVFGGGTKVTVL 262
L9        CLSWDDSLNGWVFGGGTKVTVL 262
O3        CLSWDDSLNGWVFGGGTKVTVL 262
P15      CLSWDDSLNGWVFGGGTKVTVL 262
O5       CLSWDDSLNGWVFGGGTKVTVL 262
K6       CLSWDDSLNGWVFGGGTKVTVL 262
R2       CLSWDDSLNGWVFGGGTKVTVL 262
          *****

```

Supporting Information Figure S4. Amino acid sequence alignment of V_H-V_L M8 wild type (top) to compared clones isolated from affinity maturation that contained a single V_L domain after directed evolution. Clone names are listed on the left hand side with conserved residues shown as stars, conserved mutations listed by “:”, semi-conserved by “.”, and a blank space indicates no conserved match (ClustalW).

```

VHVL M8      QVQLV ESEGG LVQP GGS LRL SCAASGFT FSSY WMSWVRQAPGKGL EGVA TIKQD GSEKYY 60
R5           -----
T6           -----
N8           -----
Q9           -----

VHVL M8      VDSVKGRITISRDN AKNSLN RQINSLRAEDTAVYYCARDRLVRETGGDYRGLDLWGQGT 120
R5           -----
T6           -----
N8           -----
Q9           -----

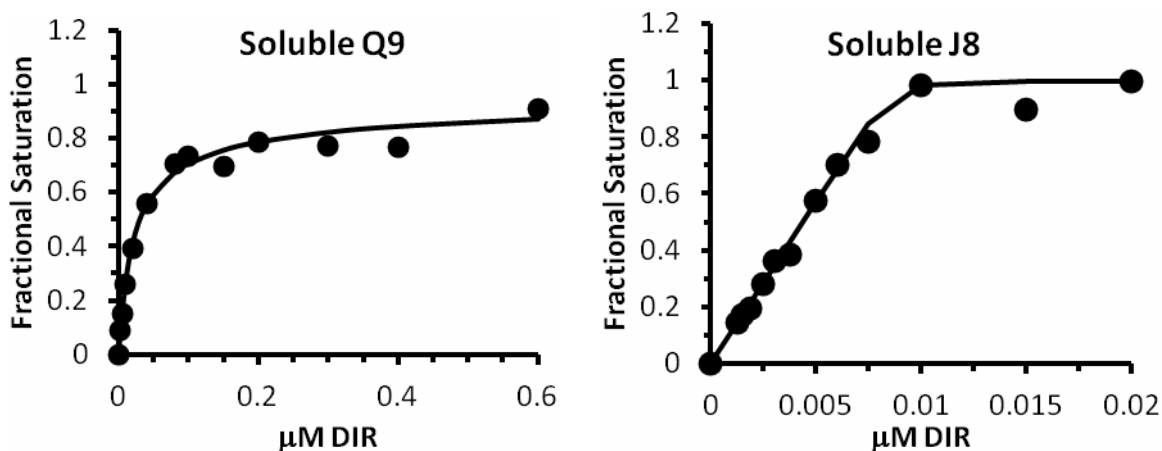
VHVL M8      VTVSSASTKGPSGILGSGGGSGGGSGGGSGQPVL TQSPSVSGTPGQKVTIFCSGSSSN 180
R5           -----GGGGSGGCGSGGGSGQPVL TQSPSVSGTPGQKVTIFCSGSSSN 43
T6           -----GGGGSCGGSGGGSGQPVL TQSPSVSGTPGQKVTIFCSGSSSN 43
N8           -----GGGGSGGGSGGGSRPALTQSPSVSGTPGQKVTIFCSGSSSN 43
Q9           -----GGGGSGGGSGGGSRPVL TQSPSVSGIPGQKVTIFCSGSSSN 43
                ***** * *****:*.***** *****

VHVL M8      VEDNSVYWYQQFP GTTPK VLIYNDDR RSSGVPDR FSGSKSGT SASLAISGLRSEDEADYY 240
R5           VEDNSVYWYQQFP GTTPK VLIYNDDR RSSGVPDR FSGSKSGT SASLAISGLRSEDEADYY 103
T6           VEDNSVYWYQQFP GTTPK VLIYNDDR RSSGVPDR FSGSKSGT SASLAISGLRSEDEADYY 103
N8           VEDNSVYWYQQFP GTTAP EVLIYNDDR RSSGVPDR FSGSKSGT SASLAISGLRPEDEADYY 103
Q9           VEGNSVYWYRQFP GTTPK VLIYNDDR RPSGVPDR LSGSKSGT SASLAISGLRPEDEADYY 103
                **.*****:*****:*.*****:*****:*****:*****

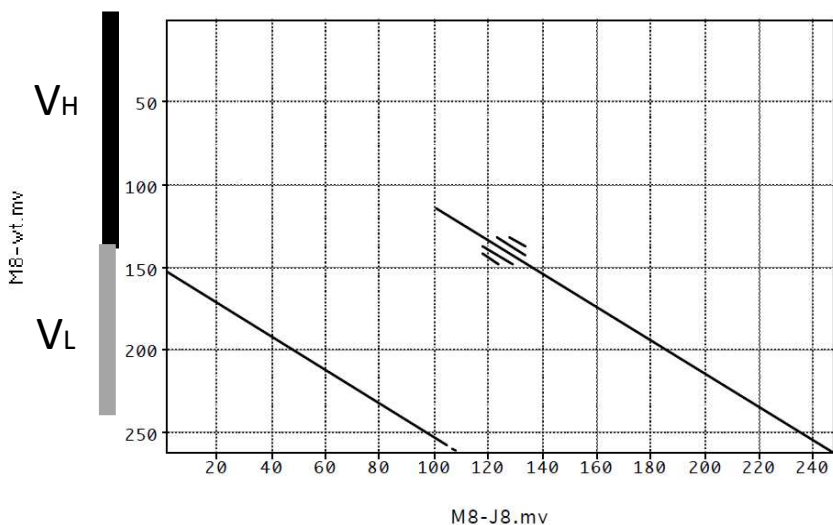
VHVL M8      CLSWDDSLNGWVFGGGTKVTVL 262
R5           CLSWDDSLNGWVFGGGTKVTAL 125
T6           CLSWDDSLNGWVFGGGTKVTVL 125
N8           CLSWDDNLNGWVFGGGTKVTVL 125
Q9           CLSWDDSLNGWVFGGGTKVTVL 125
                ***** .*****.*

```

Supporting Information Figure S5. Affinity titrations represented in Table 1. Serial dilutions of DIR were added to soluble protein in buffer for Q9 (33 nM) and J8 (9 nM) (PBS pH 7.4 with 2mM EDTA, 0.1% w/v Pluronic F-127). All measurements were performed in duplicate in 96 well black-bottom plates (Whatman) in Tecan Safire² fluorimeter and excited at 602nm. The fluorescence measurements of DIR in buffer were subtracted from the raw data prior to curve fitting. Fluorescence was recorded at 644nm and data analyzed using in-house software as described in methods section of the manuscript.



Supporting Information Figure S6. Protein scoring matrix (MacVector) of V_H-V_L M8 compared to V_L-V_L J8 pseudodimer clone from directed evolution. Scoring matrix shows identify between two light domains in V_L-V_L J8 and the V_H-V_L M8 light domain. Left-hand axis shows the relative position of the V_H or V_L domains relative to the J8 clone. Boxes along the left hand side of the diagram indicate (black) sequence homology to the M8 V_H or (grey) sequence homology corresponding to the M8V_L. Small lines represent the (G₄S) repeats in the linker region between domains.



Supporting Information Figure S7. Extension of Kabat nomenclature used for V_H-V_L M8 wild type parent clone. The residues listed below are cannot be assigned in the Kabat nomenclature. They are listed as residue L108 with a lower-case letter to indicate sequence order.

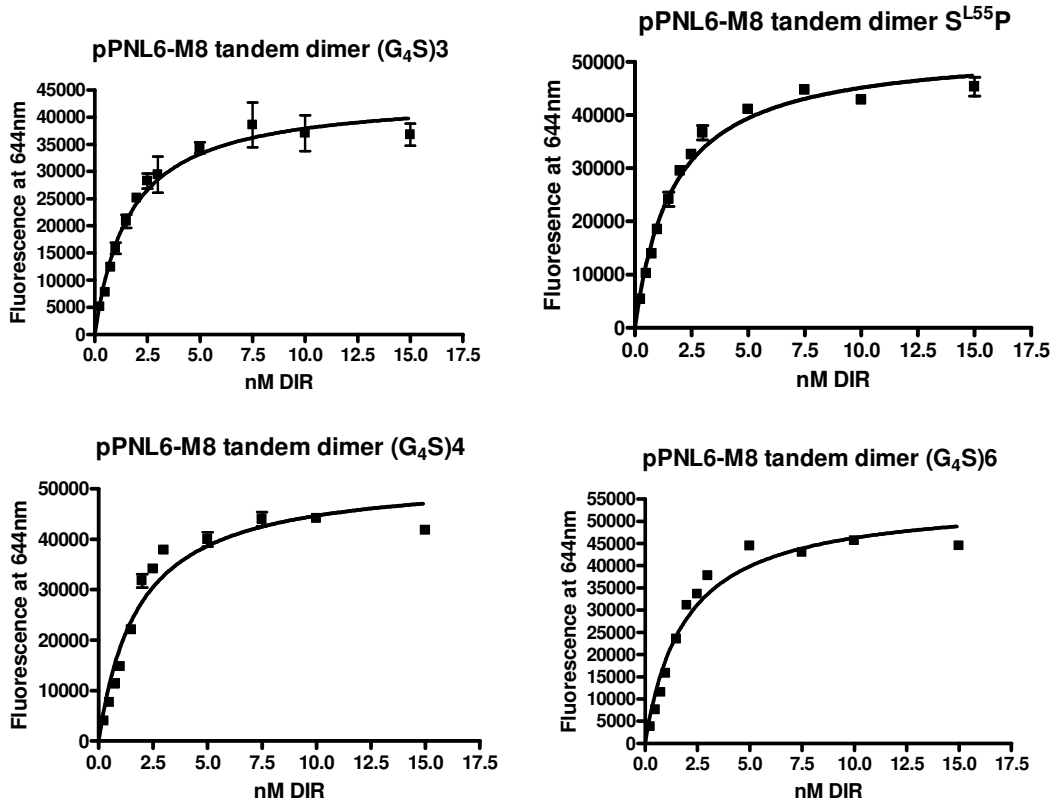
A^{L108a}, S^{L108b}, T^{L108c}, K^{L108d}, G^{L108e}, P^{L108f}, S^{L108g}, G^{L108h}, T^{L108i}, L^{L108j}, G^{L108k}

Supporting Information Figure S8. Results of altering glycine-serine rich linker length in tandem homodimers created from the M8V_L and fluorescence equilibrium affinity titrations.

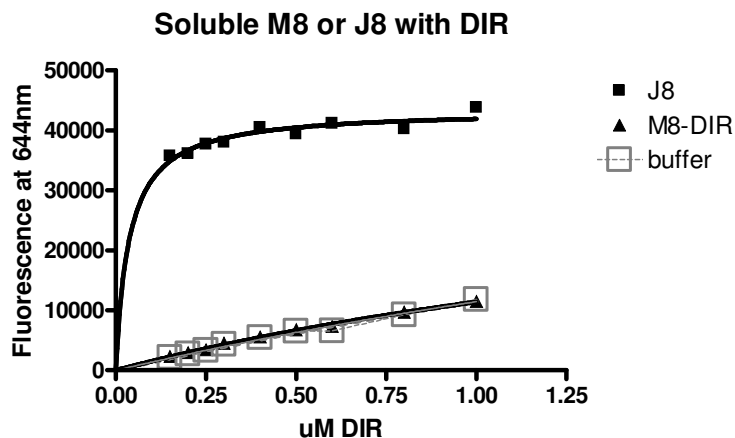
Table S8. Characteristics of covalent homodimers with different linker lengths (yeast surface).

Clone	(G ₄ S) repeats in linker	Surface K _D (nM)
dM8V _L (G ₄ S) ₃	3	1.7 ± 0.2
dM8V _L (G ₄ S) ₄	4	1.9 ± 0.3
dM8V _L (G ₄ S) ₆	6	2.0 ± 0.2
dM8V _L S ^{L55P} (G ₄ S) ₃	3	1.8 ± 0.1

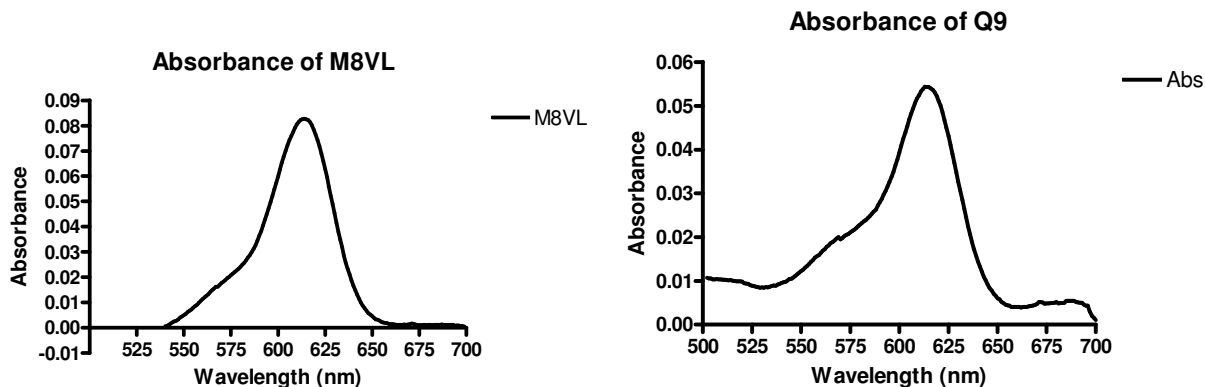
Fluorescence affinity titration represented in Table S8. Serial dilutions of DIR were added to 10⁶ yeast cells induced to display the protein of interest in buffer (PBS pH 7.4 with 2mM EDTA, 0.1% w/v Pluronic F-127). pPNL6 titles on figures indicate yeast surface display clones with the clone name after the pPNL6. The fluorescence from yeast surface proteins (black squares) are shown. All measurements were performed in duplicate in 96 well black-bottom plates (Whatman) in Tecan Safire² fluorimeter and excited at 602nm. The fluorescence measurements of DIR titrations into 10⁶ uninduced yeast cells in buffer were subtracted from the raw data prior to curve fitting. Fluorescence was recorded at 644nm and data analyzed using GraphPad fit to a one-site binding equation $y = F_{\max} * [X] / (K_d + [X])$, where [X] is DIR concentration.



Supporting Information Figure S9. Fluorescence titration curve of DIR into soluble V_H - V_L M8 (black triangle), soluble pseudodimer V_L - V_L J8 (black square) or buffer (grey triangle). Serial dilutions of DIR were titrated into 10nM soluble protein, excited at 602nm and the fluorescence recorded at 644nm on TECAN Safire² plate reader. Curves are intended to guide the eye.



Supporting Information Figure S10. Absorbance spectra for two monomeric V_L fluoromodules; 5.0uM M8 V_L with 0.5uM DIR that gives a high quantum yield (71%) and 0.5uM Q9 with 0.1uM DIR that has a low quantum yield (19%). Data obtained on a Cary 300 Bio UV-Visible spectrophotometer at 20°C.



Supporting Information S11

S11A: Effect of Protein Concentration on Data Fitting: Nine synthetic data sets were constructed using protein concentrations of 100 nM, 10 nM, and 1 nM and K_D values of 1 nM, 0.1 nM, and 0.01 nM. The error in the measured fluorescence in these data sets was 10%. Each data set consisted of 50 independent binding curves. The dependence of the χ^2 as K_D is varied provides information on the robustness of the data fitting (Figure S11A). These plots show that well defined minima in χ^2 can be obtained even if the protein concentration is considerably higher than K_D (panels A and B). In particular, protein concentrations as high as 100 nM can be used in titrations to measure K_D values as low as 1 nM. However, more robust fits are clearly obtained when the protein concentration is on the order of the K_D value (or lower). We found that the average K_D values obtained for fits which showed a well defined minimum in χ^2 for all 50 members of the data set were within a factor of 2 of the expected K_D value (see Table S11). Panel B & C (Figure S11A) indicate that at protein concentrations of ~ 1 nM (or higher), K_D values less than 0.1 nM cannot be reliably obtained by fitting.

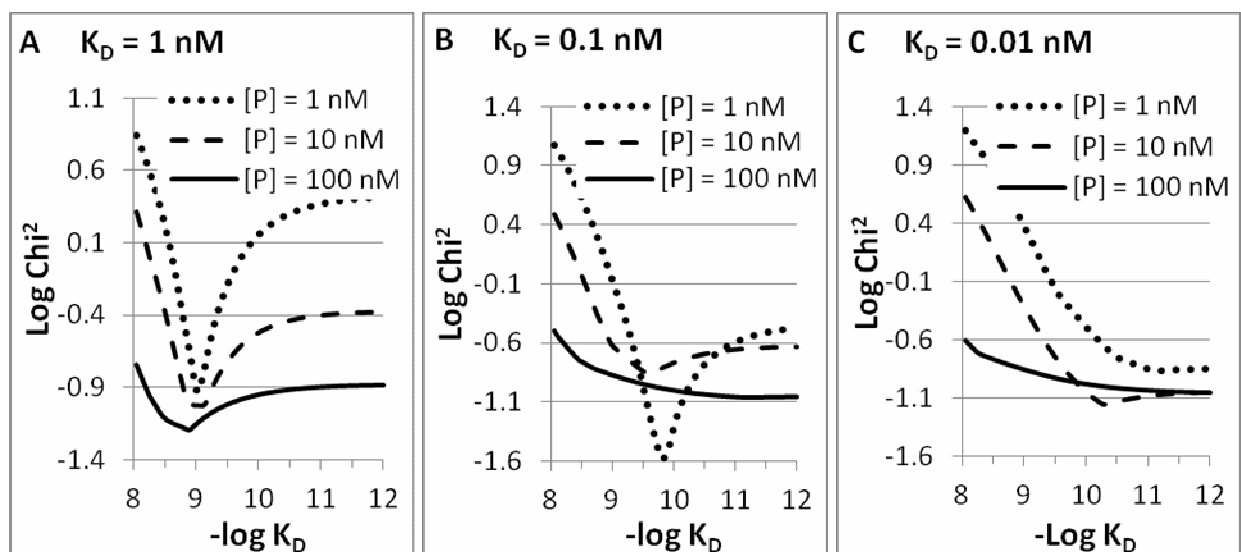
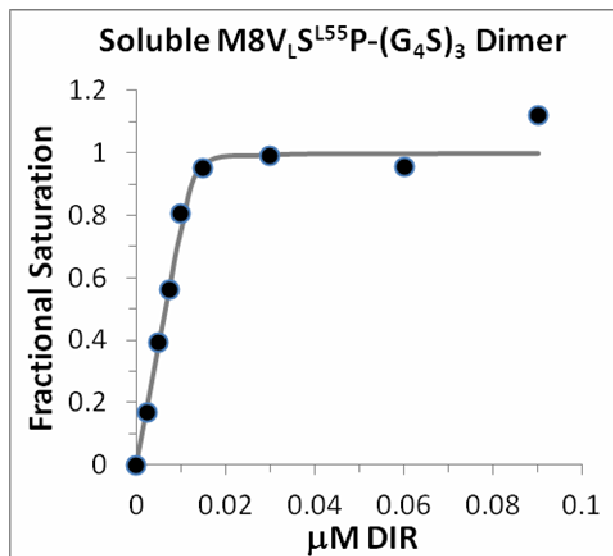
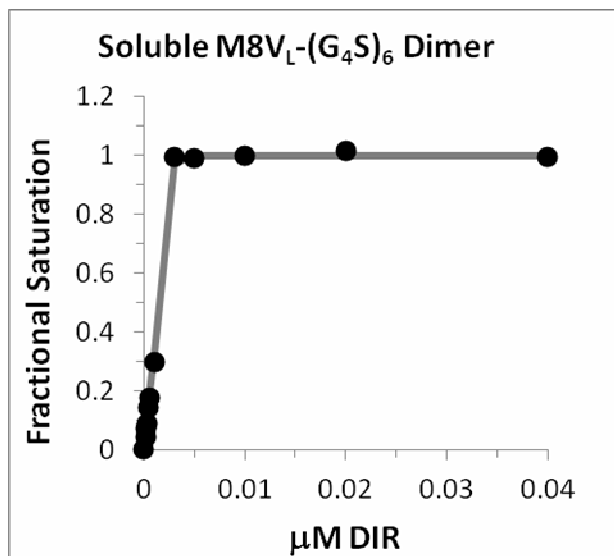
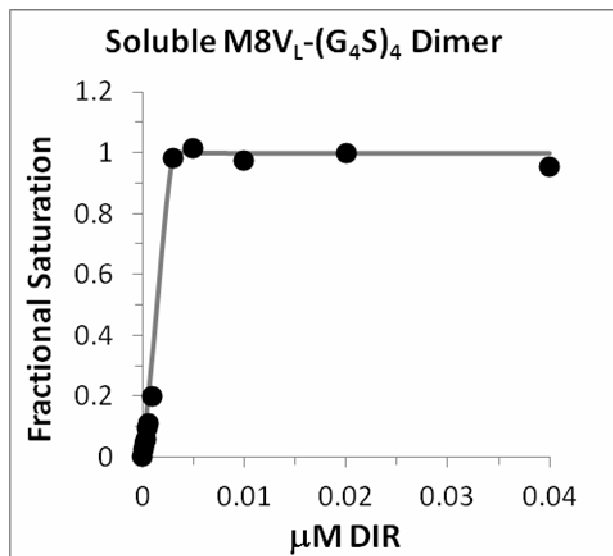
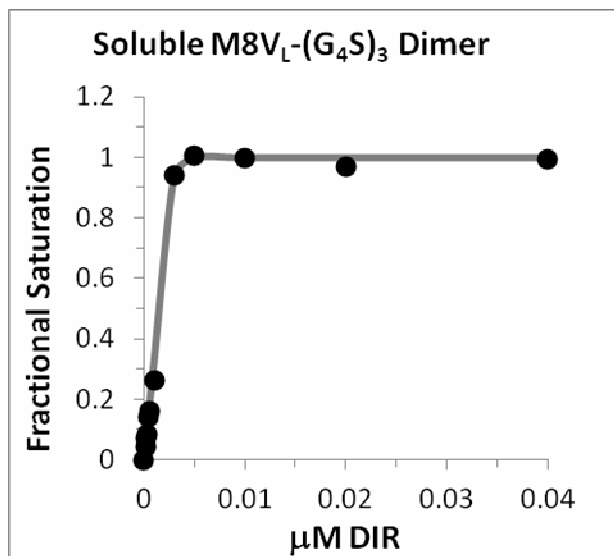


Figure S11A. The effect of varying protein concentration on the ability to obtain K_D values from data fitting. For each of the K_D values (A=1.0, B= 0.1, C= 0.01 nM) and protein concentrations (100, 10, 1 nM), a total of 50 synthetic data sets were constructed assuming an error of 10% in the measurement of the fluorescence signal. Plotted curves are a representative plot of the log of the square of the difference between the actual and predicted data (χ^2) for one of the 50 data sets associated with each condition. Panels A and B indicate that a clear minima in the χ^2 value can be observed for measurements where the protein concentration is 10 fold higher than the K_D . Panel C shows that reliable values for K_D values less than ~ 0.01 nM cannot be obtained if the protein concentration is 1 nM or higher.

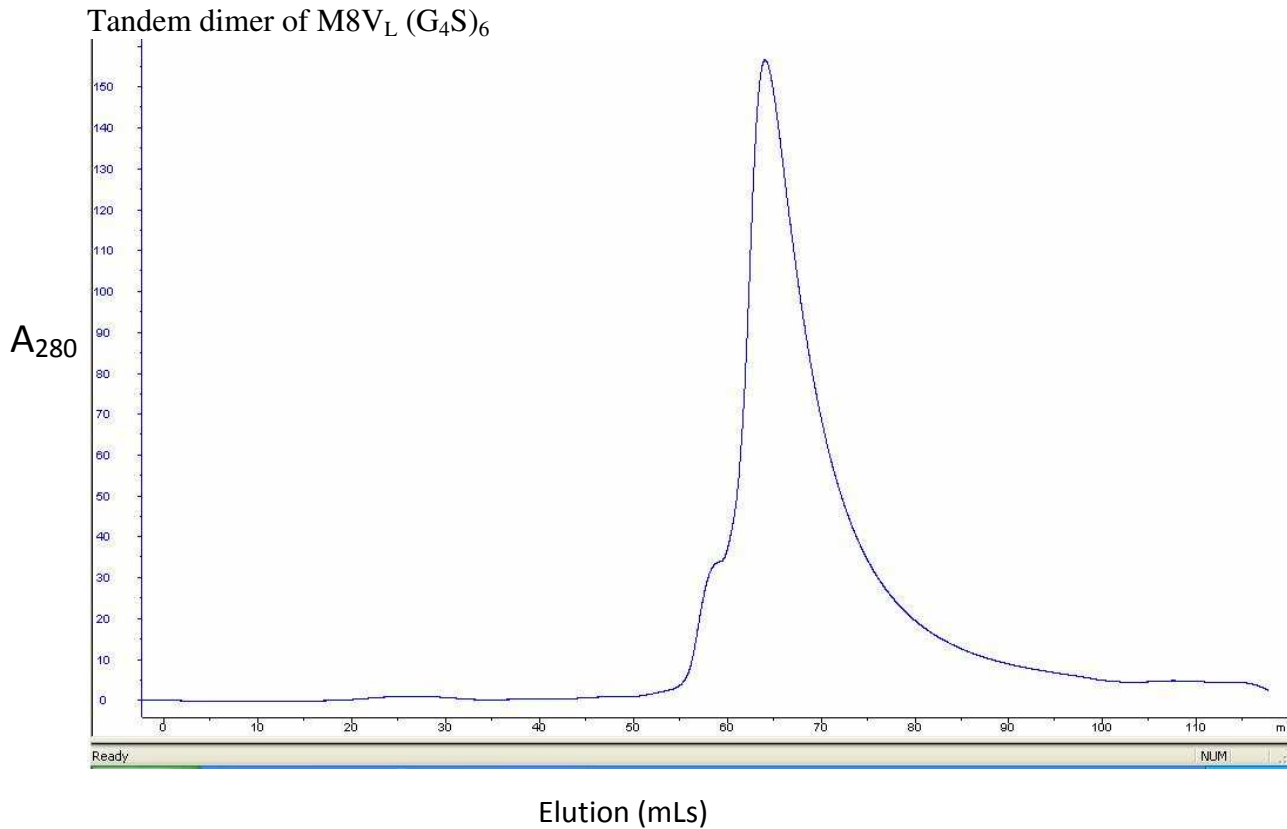
Table S11 – Effect of Protein Concentration on Fitting Accuracy.

K_D (Expected)	Fitted K_D		
	[P]=100 nM	[P]=10 nM	[P]=1 nM
1.00 nM	1.42 ± 1.00	0.94 ± 0.27	1.00 ± 0.09
0.10 nM	No χ^2 minimum.	0.18 ± 0.10	0.150 ± 0.030

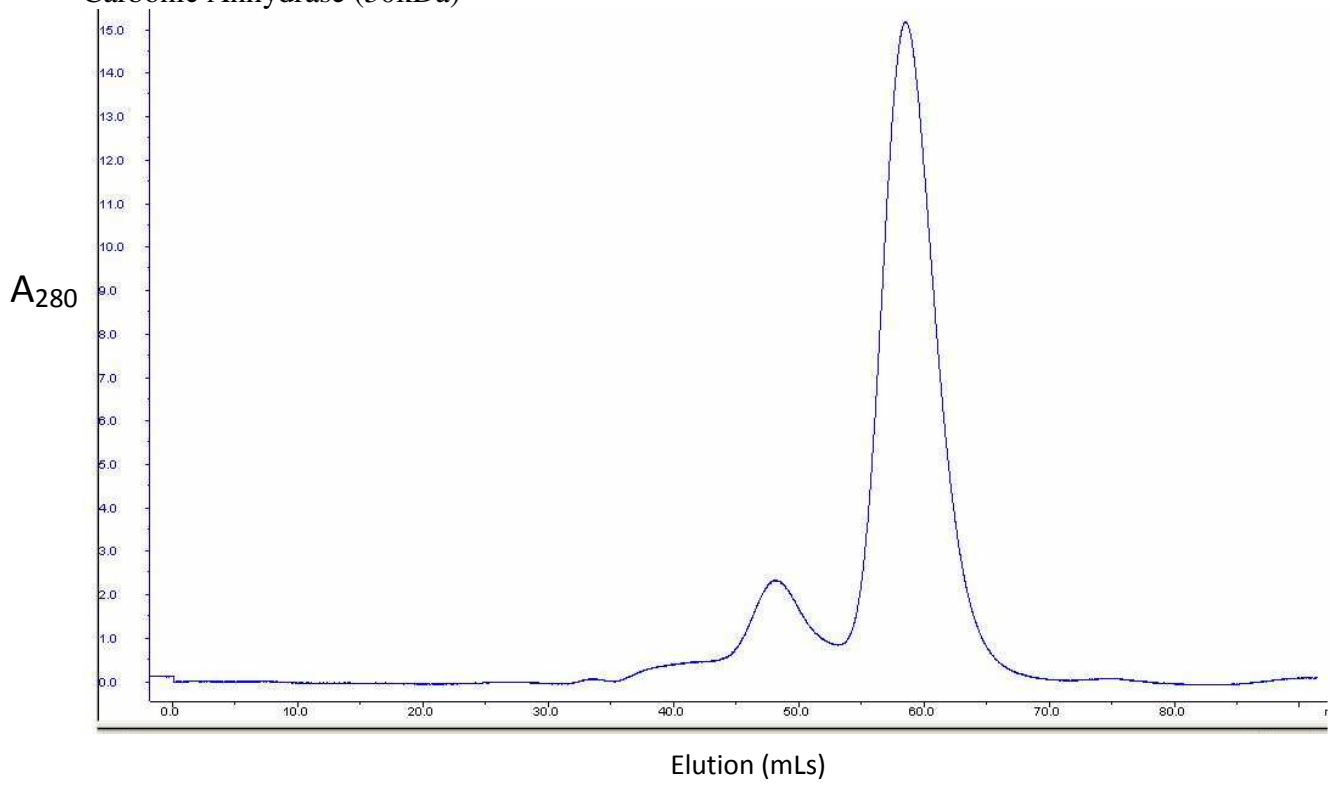
S11B: Fluorescence affinity titrations represented in Table 2 for synthetic dimers of M8V_L and M8V_LS^{L55}P. These were performed in PBS, pH 7.4, with 2mM EDTA, 0.1% w/v Pluronic F-127 by titrating DIR into protein solutions. Concentrations of proteins were 3nM, 3nM, 3nM, and 12 nM for M8V_L(G₄S)₃, M8V_L(G₄S)₄, M8V_L(G₄S)₆, M8V_LS^{L55}P, respectively. All measurements were performed in triplicate in 96 well black-bottom plates (Whatman) in Tecan Safire² fluorimeter and excited at 602nm. Fluorescence was recorded at 644nm and data, corrected for background fluorescence in the absence of protein, and fit to a single binding site using the quadratic equation with in-house software. The solid grey line shows the best fit.



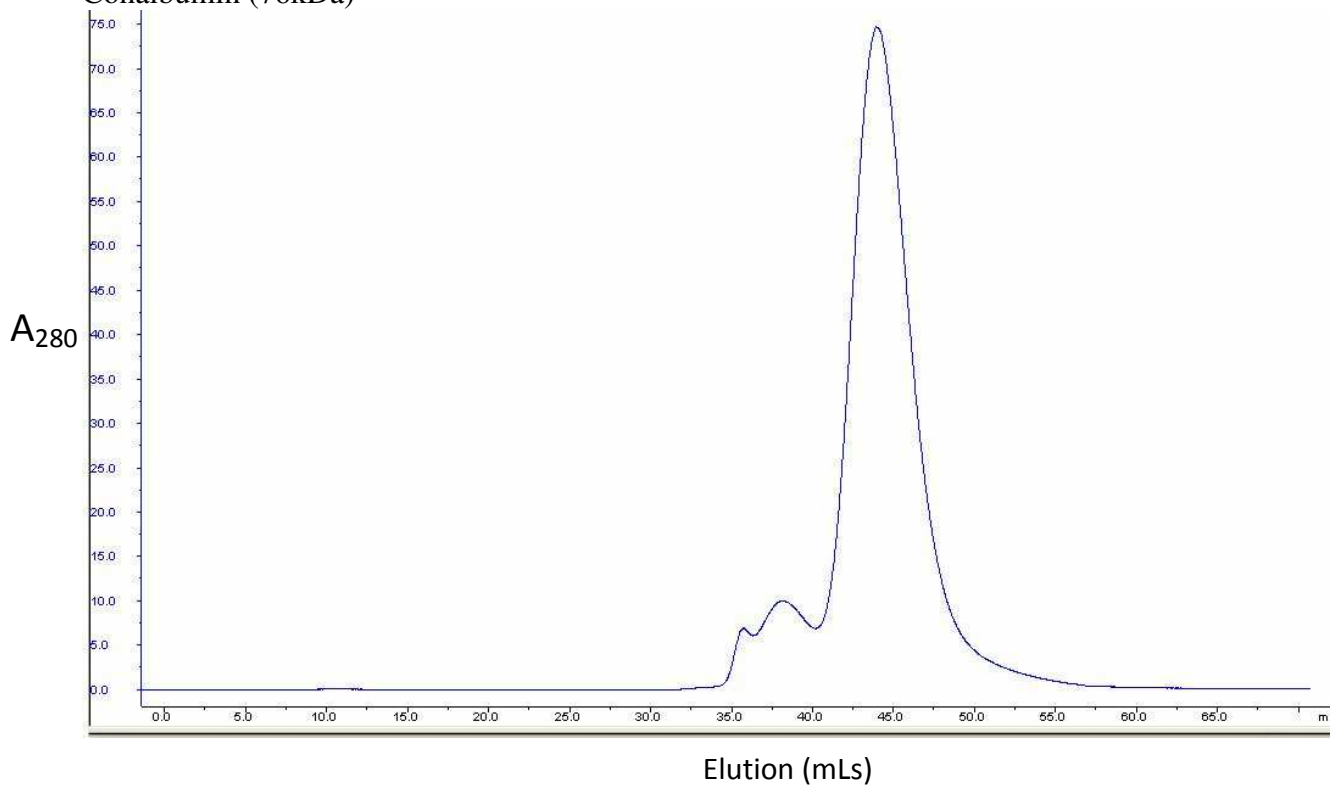
Supporting Information S12. Size exclusion analysis of the tandem homodimer M8V_L with (G₄S)₆ linker repeats. Four milligrams of purified protein was injected into a HiPrep 16/60 Sephacryl S-100 column (GE Healthcare) in buffer (10mM Tris pH 8.0, 300mM NaCl) run at 1mL/min.. The single peak of tandem dimer M8V_L (G₄S)₆ corresponds to a molecular weight of 26kDa (elution of 65mLs). For comparison two molecular weight standards are shown, conalbumin 76kDa (elution 45mLs) and carbonic anhydrase B 30kDa (elution 60mLs).



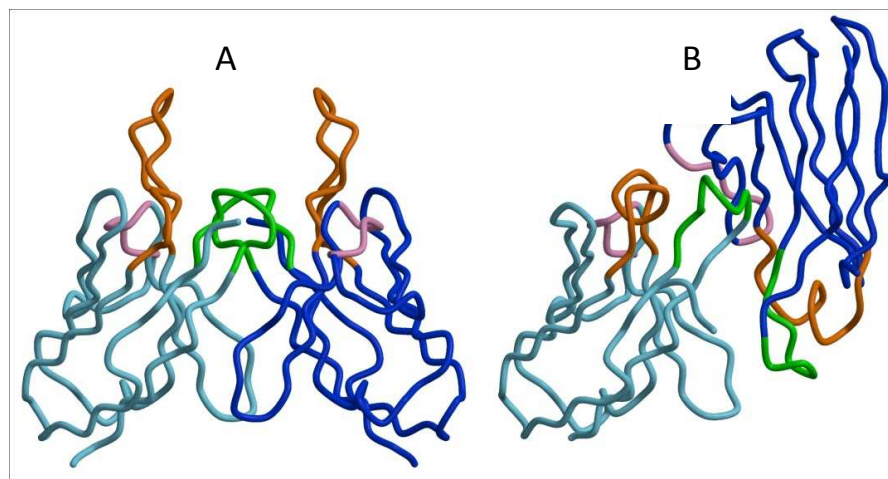
Carbonic Anhydrase (30kDa)



Conalbumin (76kDa)



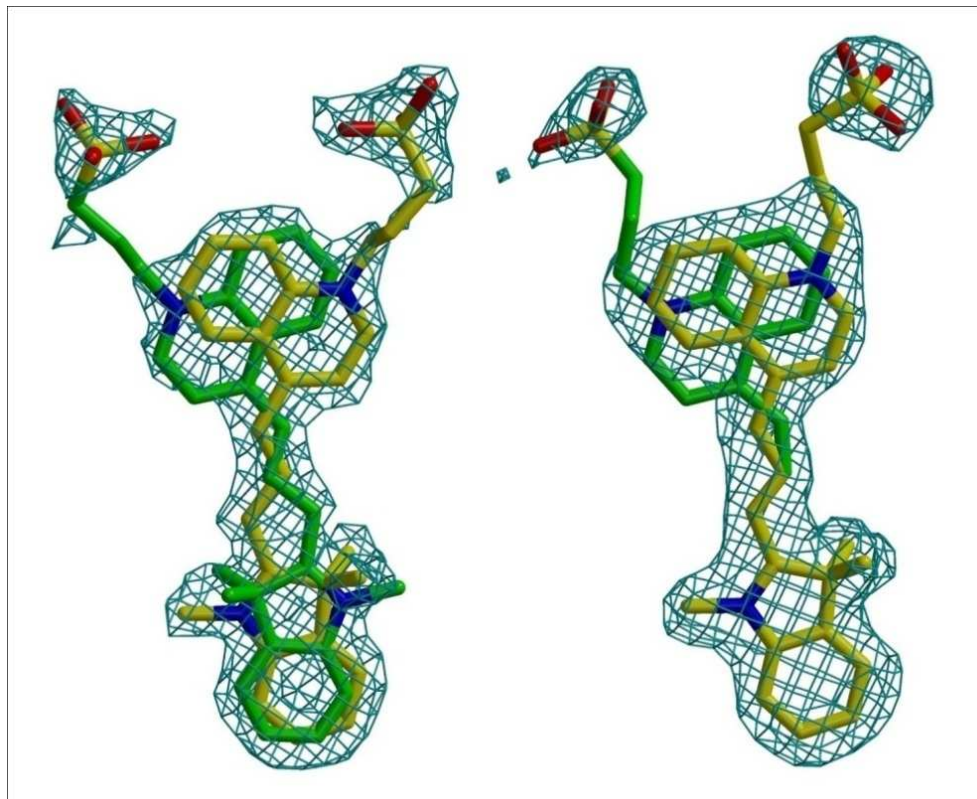
Supporting Information Figure S13. Comparison of V_L dimeric arrangement. (A) The ‘typical’ light chain dimer LEN has a V_L - V_L arrangement very similar to that seen in a Fab V_L - V_H variable domain. (B) The $M8V_L S^{L55}P$ dimer is shown, oriented with the A chain (light blue) superimposed on the A chain of LEN. The B chain (dark blue) is rotated by 133° from the position of the B chain in LEN. The B chain of the $M8V_L$ structure (not shown) is rotated 131° from the position in LEN.



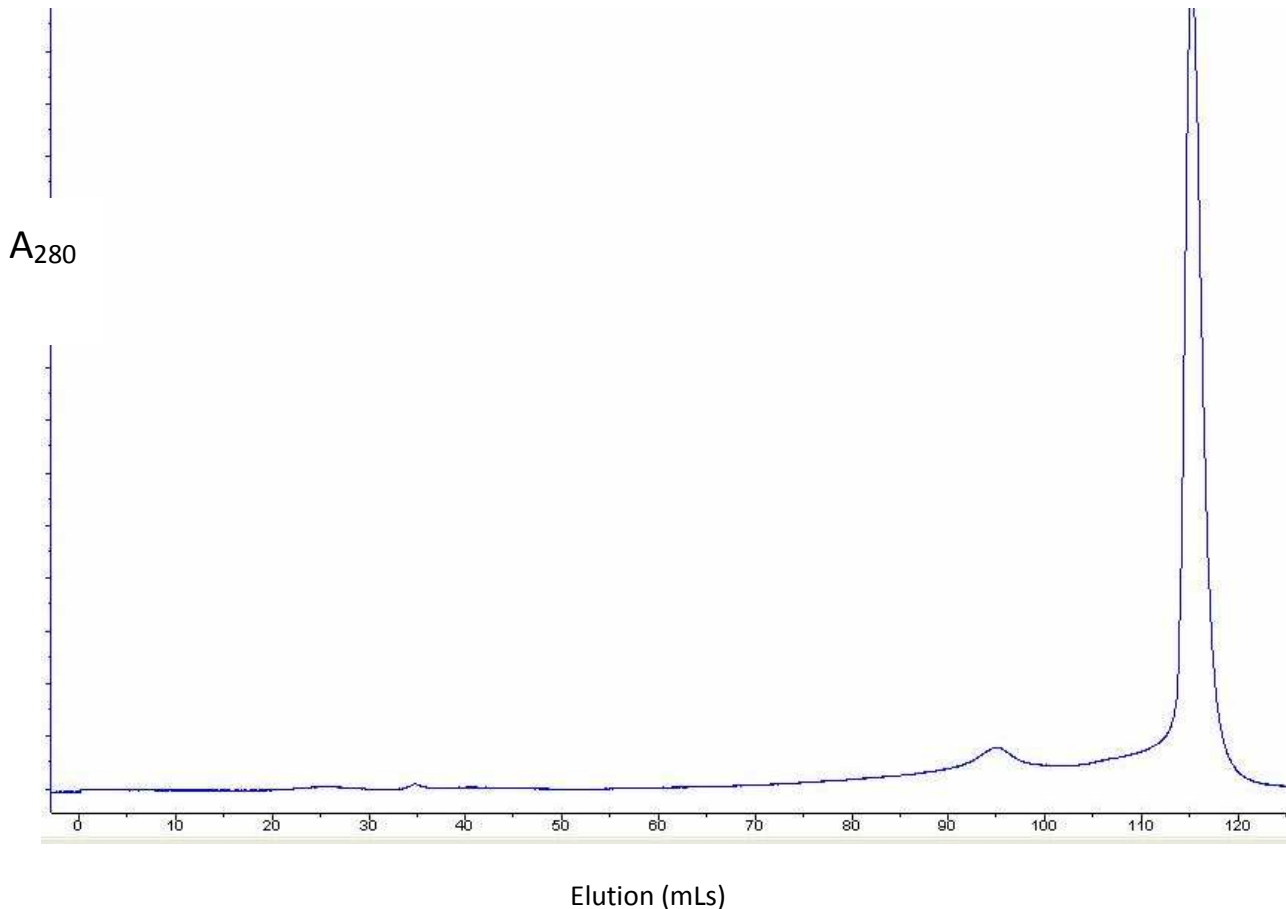
Supporting Information Table S14. Table of angles calculated between key contact residues and different functional groups of DIR in two conformations. Also shown are distances between key contact residues and the different functional groups of DIR. The DIR atoms used to estimate the plane and center of gravity of the quinoline ring were C14, C15, C19, C20, C21, C22. This is the 6-atom ring closest to the Tyr^{L49} ring. DIR atoms used for the indole ring plane and center of gravity were N7, C, C2, C3, C8, C9, C30, C31, C32. The Tyr and Phe ring planes and centers of gravity used the 6 atoms of the main ring, and the Trp ring plane and center of gravity was calculated using all indole atoms. Distances are between the centers of gravity of the ring systems.

Table S14. Angles and distances between aromatic residues and DIR									
		M8V _L				M8V _L S ^{L55} P			
		Angle (°)		Distance (Å)		Angle (°)		Distance (Å)	
DIR atoms	FAP atoms	DIR conf. 1	DIR conf. 2	DIR conf. 1	DIR conf. 2	DIR conf. 1	DIR conf. 2	DIR conf. 1	DIR conf. 2
quinoline	Tyr49A	5.0	7.6	4.0	3.6	7.1	10.7	3.9	3.7
quinoline	Tyr49B	10.4	6.5	3.7	4.1	11.3	7.6	4.3	4.2
indole	Tyr34A	36.4	36.7	5.8	5.9	31.7	31.7	5.6	5.6
indole	Tyr34B	34.1	32.9	5.9	5.8	36.3	36.3	6.1	6.1
indole	Trp96A	75.4	74.0	5.6	5.5	78.6	78.6	5.5	5.5
indole	Trp96B	71.1	70.3	5.7	5.7	72.2	72.2	5.6	5.6
indole	Phe98A	67.3	66.8	6.7	6.8	67.6	67.6	6.9	6.9
indole	Phe98B	64.1	62.7	7.0	6.9	65.7	65.7	6.8	6.8

Supplemental Information S15. Electron density for DIR ligands. (a) Electron density (1σ contour) in the M8V_L complex shows two alternate conformations for DIR that are related by the approximate non-crystallographic 2-fold symmetry. (b) Electron density (1σ contour) for DIR in the M8V_LS^{L55}P complex shows one conformation for the indole ring, and two conformations for the quinoline ring that are related by the approximate non-crystallographic 2-fold axis.



Supporting Information Figure S16. Gel filtration chromatography of purified M8V_L monomer protein on Sephacryl S-100 column (GE Healthcare) with a 120mL column volume. The M8V_L elutes in a large peak at approximately 116mLs, an elution volume much reduced when compared to low molecular weight kit of protein gel filtration standards (GE Healthcare). This unusual elution pattern was not altered by several buffer conditions tested.



Supporting Information Figure S17. NMR data of mean T_2 relaxation times, in addition to the theoretical and experimentally derived global correlation times (τ_m).

	M8V _L	M8V _L in the presence of DIR
Mean T_2 (ms)	95.80	57.17
Theoretical τ_m (ns)	9.36	16.38
Experimental τ_m (ns)	9.90	15.87